The Journal of Neuroscience, November 15, 1998, *18*(22):9489–9499

Functional Streams and Local Connections of Layer 4C Neurons in Primary Visual Cortex of the Macaque Monkey

N. Harumi Yabuta and Edward M. Callaway

Systems Neurobiology Laboratories, The Salk Institute for Biological Studies, La Jolla, California 92037

The primate visual system is composed of multiple, functionally specialized cortical areas. The functional diversity among areas is thought to reflect different contributions from early parallel visual pathways to the area V1 neurons providing input to "higher" cortical areas. The M pathway is believed to provide information about motion and contrast, via layer 4B of V1, to dorsal visual areas. The P pathway is believed to provide information about shape and color, via layer 2/3 of V1, to ventral visual areas, with specialized contributions from cytochrome-oxidase (CO) blob versus interblob neurons. However, the detailed anatomical relationships between the M and P pathways and the neurons in V1 that provide input to higher extrastriate cortical areas are poorly understood. To study these relationships, spiny stellate neurons in the M- and P-recipient layers of V1, 4Cα and 4Cβ, respectively, were intracellularly labeled, and their axonal and dendritic arbors were reconstructed. We find that neurons with dendrites in upper layer 4Cα project axons to layer 4B and CO blobs in layer 2/3, thus relaying M input to these regions. Other neurons in lower layer 4Cα provide M input to interblobs. These cells have either (1) dendrites restricted to lower layer 4Cα and axons specifically targeting layer 2/3 interblobs, or (2) dendrites in lower 4Cα and 4Cβ and axons targeting blobs and interblobs. P-recipient layer 4Cβ neurons have dense axonal arbors in both blobs and interblobs but not layer 4B. Quantitative analyses reveal that 4Cα cells provide approximately five times more synapses than 4Cβ cells to layer 4B, whereas 4Cβ cells provide five times more synapses than 4Cα cells to layer 2/3. These observations imply that M input is dominant in layer 4B. In layer 2/3, both blobs and interblobs receive M and P input, but the P input is dominant, and M input to interblobs derives exclusively from a subpopulation of M afferents that targets lower 4Cα, not from afferents targeting only upper 4Cα (cf. Blasdel and Lund, 1983). We speculate that the M and P pathways to interblobs are "X-like" linear systems, whereas blobs also receive nonlinear "Y-like" M input.

Key words: functional streams; local circuits; macaque; primary visual cortex; primate; V1

The relative contributions of the functionally distinct M and P pathways are believed to be important determinants of the functional differences between extrastriate cortical areas (Livingstone and Hubel, 1988; for review, see Merigan and Maunsell, 1993). Nevertheless, the actual relationships between the M and P streams and V1 neurons projecting to extrastriate cortex are poorly understood. We have addressed these relationships by studying spiny stellate neurons in layer 4C of V1, because they lie at the heart of the problem; they provide a direct link from LGN afferents to extrastriate projection neurons.

In the retino–geniculo–cortical system, parallel M and P pathways converge on V1, where they segregate their inputs into layers 4Cα and 4Cβ, respectively (Hubel and Wiesel, 1972; Hendrickson et al., 1978; Blasdel and Lund, 1983). Layer 4C neurons connect to neurons in more superficial layers (layers 2–4B) (for review, see Callaway, 1998), and these superficial neurons provide output, both directly and indirectly, to functionally specialized extrastriate cortical areas (for review, see Felleman and Van Essen, 1991). Specifically, neurons in layer 4B of V1 provide direct and indirect input to dorsal visual areas believed to be involved in computations about spatial relationships and motion in visual scenes. Layer 2/3 can be subdivided into cytochrome-oxidase (CO)-rich blob and interblob regions, which project in parallel to ventral visual areas specialized for visual object identification (for review, see Desimone and Ungerlieder, 1989; Felleman and Van Essen, 1991).

Based on differences in response properties, it has been suggested that blobs might receive input from both the M and P pathways, whereas interblobs are influenced primarily by the P pathway (Livingstone and Hubel, 1988; Edwards et al., 1995). In particular, blob neurons have better contrast sensitivity and are, on average, selective for lower spatial frequencies than are interblob neurons (Tootell et al., 1988a,b,c; Edwards et al., 1995), properties more like those of magnocellular LGN neurons or M-recipient layer 4Cα cells than neurons in the P pathway (Kaplan and Shapley, 1982; Blasdel and Fitzpatrick, 1984). These relationships received anatomical support when Lachica et al. (1992) showed that M-recipient layer 4Cα neurons were retrogradely labeled after tracer injections in blobs but not interblobs. Layer 4Cβ neurons were labeled after injections in either region (but see Yoshioka et al., 1994).

Although these findings suggest a lack of M input to interblobs, there is other evidence for M input to interblobs. Neuronal activity is decreased for both blob and interblob neurons after inactivation of either M or P layers of the LGN (Nealey and Maunsell, 1994), and some interblob cells are selective for low spatial frequencies (Edwards et al., 1995), a trait suggestive of M input.

Received July 1, 1998; revised Aug. 24, 1998; accepted Aug. 26, 1998.

This work was supported by National Institutes of Health Grant EY10742. We thank Jami Dantzker for assistance in labeling neurons and Atomu Sawatari for tissue processing. Atomu Sawatari and Drs. Amy Butler, Francis Crick, and Lisa Croner provided valuable comments on earlier versions of this manuscript.

Correspondence should be addressed to Edward M. Callaway, Systems Neurobiology Laboratories–C, The Salk Institute for Biological Studies, 10010 North Torrey Pines Road, La Jolla, CA 92037.

Our aim therefore is to reveal how the type of LGN input to layer 4C neurons is related to their output to layer 4B and to the blob and interblob regions of layer 2/3. We have directly assessed these relationships by reconstructing the axonal and dendritic arbors of intracellularly labeled layer 4C spiny stellate neurons. The relationships of their dendritic arbors to layers 4Cα and 4Cβ reveal the likely contributions of the M and P pathways to their input. The patterns of axonal arborization of the same cells reveal their potential contributions to neurons in more superficial layers.

In addition to identifying neurons with axonal projection patterns predicted from retrograde labeling studies, we have identified sources of M input to interblobs and cell types that were not anticipated. As expected, we found layer 4Cα cells projecting specifically to blobs and layer 4B and found layer 4Cβ cells projecting to blobs and interblobs, but we also found three other cell types in layer 4Cα. One cell type has axons restricted to layer 4C, whereas the other two can provide M input to interblobs. Cells providing M input to interblobs either have narrowly stratified dendrites restricted to lower 4Cα and dense axons specifically targeting layer 3 interblobs, or they have dendrites in lower 4Cα and 4Cβ and axons targeting blobs and interblobs. These findings point out the importance of considering functional differences between the type of M input to upper versus lower layer 4Cα (cf. Blasdel and Lund, 1983).

MATERIALS AND METHODS

Twenty-three spiny stellate neurons with somata in layer 4C of the primary visual cortex of rhesus macaque monkeys were intracellularly labeled with biocytin, and their axonal and dendritic arbors were reconstructed. The neurons in our sample were labeled in V1 brain slices prepared from six rhesus macaque monkeys (*Macaca mullata*). The ages, sex, and number of cells labeled from each animal were as follows: (1) 10 months, male, one cell; (2) 13 months, male, eight cells; (3) 15 months, male, three cells; (4) 15 months, male, four cells; (5) 16 months, female, two cells; (6) 17 months, male, five cells. Other brain slices prepared from the same animals were used for unrelated studies.

The methods used for cell labeling and reconstruction have been described in detail previously (Callaway and Wiser, 1996; Wiser and Callaway, 1996; Yabuta and Callaway, 1998). Briefly, living coronal brain slices were prepared from V1 and held in interface chambers. They were then transferred to a recording chamber in which whole-cell patch electrodes were used to record intracellularly from layer 4C neurons and fill them with biocytin. The slices were then fixed and double stained for CO to reveal laminar boundaries and CO blobs and with biocytin to reveal neuronal processes.

Spiny stellate neurons with axonal processes that could be followed to their ends or until they left the plane of the brain slice without fading were selected for further analysis. Photographs of a typical cell are shown in Figure 1. The axonal and dendritic arbors of each cell were reconstructed using a light microscope with Neurolucida, a computerized camera lucida system (MicroBright Field Inc.), and a 60×, 1.4 NA oil immersion microscope objective. Synaptic boutons were identified using a 100× objective when necessary, and their positions were marked. *En passant* synaptic boutons were identified as periodic axonal swellings, and boutons *terminaux* were identified as spine-like protrusions with a bulbous ending. Laminar boundaries revealed by the pattern of CO staining were also identified, as were the locations of the centers of CO blobs (see Fig. 1). After neuronal reconstruction, sections were stained for Nissl substance with thionin to identify the layer 4Cα/4Cβ border.

Rather than assigning the locations of synaptic boutons to discrete blob or interblob compartments, our quantitative analyses were based on the distance of each synaptic bouton to the nearest blob center. The centers of CO blobs were marked as a straight line running through the darkest staining region of each blob from layer 1 to layer 4A. The distances of synaptic boutons from blob centers were calculated as the shortest distance from each bouton to a point on the line indicating the nearest blob center.

This method of analysis was chosen because (1) there likely are not sharp transitions that distinguish blobs from interblobs as discrete binary entities, and (2) the sizes and spacing of blobs are highly variable. Because the density of CO staining changes gradually, the location of any distinct boundary drawn between blobs and interblobs is necessarily subjective (Edwards et al., 1995). Furthermore, functional transitions (Livingstone and Hubel, 1984; Edwards et al., 1995) and the relationships of horizontal connections to blobs (Yabuta and Callaway, 1998) shift gradually with respect to blob centers. Therefore, describing the distance of synaptic boutons to blob centers is advantageous, because it provides a more objective description and also has the potential to reveal any trends in the data that are gradual rather than discrete. For illustrative purposes, we have nevertheless marked transitions from blobs to interblobs in our neuronal reconstructions.

RESULTS

Twenty-three spiny stellate neurons with somata in layer 4C were intracellularly labeled with biocytin in living coronal brain slices prepared from area V1 of six juvenile rhesus macaque monkeys (*M. mullata*) (Fig. 1). The axonal and dendritic arbors of each cell were reconstructed, and the positions of all synaptic boutons were marked to allow quantitative analyses.

For descriptive purposes, we divide the 23 labeled cells into groups on the basis of their cell body positions, patterns of dendritic arborization, and/or patterns of axonal arborization. We are primarily interested in the relationships of neurons to input from different types of LGN afferents. We therefore distinguish three layer 4C zones, each of which receives different geniculate contributions. Blasdel and Lund (1983) identified two types of M afferents, one targeting only upper layer 4Cα and the other targeting both upper and lower 4Cα; P afferents target layer 4Cβ (Hubel and Wiesel, 1972; Hendrickson et al., 1978). We therefore distinguish upper layer 4Cα from lower 4Cα, a narrow zone at the bottom fifth of 4Cα. Sixteen of the neurons in our sample have cell bodies in layer 4Cα: 10 in upper 4Cα and six in lower 4Cα. The percentage in lower 4Cα is higher than expected by chance, because we explicitly targeted many of our electrode penetrations to this narrow zone. Seven neurons have somata in layer 4Cβ.

Upper 4Cα neurons

Reconstructions of neurons with somata in upper layer 4Cα are illustrated in Figures 2 and 3, *B* and *C*. We distinguish two cell types with somata in upper 4Cα. The most common cell type at this depth (8 of 10 cells) has axonal arbors projecting to layers 2–4B (Fig. 2). The other type (2 of 10 cells) only rarely extends axons above layer 4C (Fig. 3*B*,*C*). Two of the six lower 4Cα cells are also of the latter type (Fig. 3*A*) and will also be considered here.

Layer 4Cα cells without axons in superficial layers are distinct from those projecting to layer 4B and above. For example, the 11 layer 4Cβ and lower 4Cα cells in our sample (see below) that project to layers 3B and 4A (and not 4B) all have distinctive rising axon collaterals, extending nearly vertically above the cell body (Figs. 4, 5). None of the four cells lacking superficial projections has this type of axon collateral. Instead, any rising axon collaterals are configured like those of the upper 4Cα cells with superficial projections (Fig. 2). Nevertheless, these cells differ not only in their superficial projections but also in their projections to deeper layers. Upper layer 4Cα cells projecting to layers 2–4B usually have axonal branches in layer 5 (seven of eight cells), while all four cells projecting only as high as layer 4C clearly lack layer 5 branches (compare Figs. 2 and 3). Finally, the lack of superficial projections does not result from the cutting of axon collaterals during slice preparation. With few exceptions, the rising axons of cells without projections to superficial layers end within the plane of the brain slice.

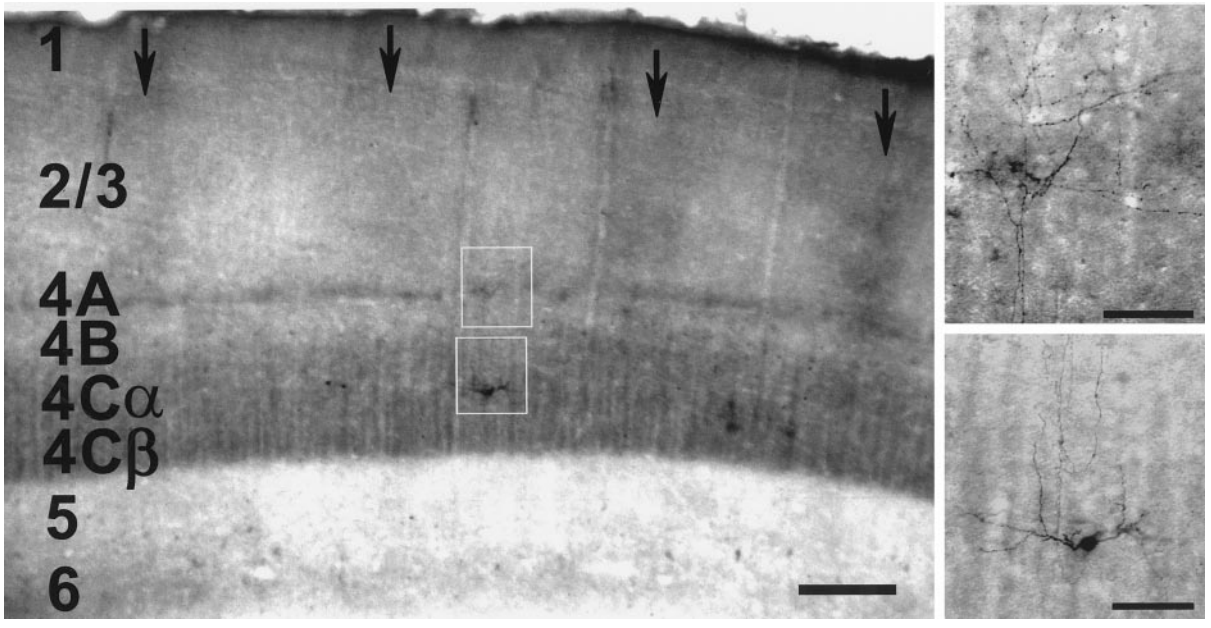

Figure 1. Photomicrographs of a section from a V1 brain slice containing an intracellularly labeled layer 4C spiny stellate neuron. The section is double stained for biocytin to reveal the labeled neuron and CO to reveal laminar boundaries and blobs. In the low-power view to the *left*, the CO blobs (indicated by *arrows*) and laminar pattern of CO staining (layers indicated by *numbers* to the *left*) are clearly visible. The *white boxes* outline regions of the section corresponding to the higher-magnification micrographs shown at the *right*. The *top box* corresponds to the *top right* micrograph and the *bottom box* to the *bottom right* micrograph. The *top right* micrograph illustrates the densely labeled axonal processes arborizing in layers 4A and 3B. The *bottom right* micrograph illustrates the cell body, dendrites, and rising axonal processes of the biocytin-labeled neuron. The neuron is located in lower layer 4Cα, has narrowly stratified dendrites confined to lower 4Cα, and has an axonal arbor specifically targeting an interblob in layer 3. The reconstruction of this neuron is shown in Figure 4*B*. Scale bars: *left panel*, 200 μm; *right panels*, 50 μm.

Although layer 4Cα cells without superficial projections differ from other upper 4Cα cells in their projections to layer 5, both cell types can have axonal branches in layer 6 (five of eight superficially projecting cells; two of four cells that lack superficial projections). Quantitative differences in the laminar distributions of the synaptic boutons from these cells are illustrated in Figure 6*A*. The two types of 4Cα cells (Fig. 6*Ai*,*Aii*) provide similar numbers of synaptic boutons per cell within layers 4C and 6, but the cells with projections to more superficial layers have far more boutons in layer 5.

Upper layer 4Cα cells with axonal arbors in layer 3 preferentially target blobs. In our sample, these projections are provided by seven upper 4Cα cells, with projections to both layers 2/3 and 4B (Fig. 2*A–C*). [One of the eight upper 4Cα cells with superficial projections extends axons only to layer 4B (Fig. 2*D*).] Preferences of axonal arbors for blob regions are apparent from visual inspection of the reconstructions (Fig. 2*A–C*). Six of the seven cells with axons in layer 3 have blob preferences similar to those illustrated. The one remaining cell has axonal arbors in layer 4B and in an interblob zone in layer 3 (data not shown). The axons from this one cell contribute 225 synaptic boutons to layer 2/3; for comparison, the cell illustrated in Figure 2*B* has 246 boutons in layer 2/3, and the average for all seven cells is 283 boutons per cell.

To quantify the overall contributions of these seven cells to blob versus interblob regions, the distance of every synaptic bouton within layer 2/3 (1979 boutons from seven cells) to the center of its nearest blob was measured (see Materials and Methods). These values were pooled for all seven cells and plotted in the histogram shown in Figure 6*Bii*. More than half of all layer 2/3 synaptic boutons from these cells are located within 50 μm of the center of a blob; more than 80% are within 100 μm. Virtually all of the remaining boutons are contributed by the cell with axons preferentially in an interblob (see above), and these account for all of the boutons in the secondary peak at >200 μm from blob centers.

Lower 4Cα neurons

Three cell types were distinguished in lower layer 4Cα. Of six cells, two have axons that do not extend above layer 4C (Fig. 3*A*). These cells have been described along with similar cells in upper 4Cα (see above). It is noteworthy, however, that these two cells differ from those in upper 4Cα in that both cells have dendritic branches extending into layer 4Cβ and axonal branches at the bottom of layer 4Cβ.

The remaining four cells with somata at the bottom of layer 4Cα have axons extending through layer 4B and arborizing in layers 4A and 3; they have only sparse axonal arbors in deeper layers (Fig. 4). Two of these four cells have narrowly stratified dendritic arbors that do not extend into layer 4Cβ (Figs. 1, 4*A*,*B*). They are therefore likely to sample input from M afferents that target lower 4Cα but not from P afferents or M afferents that target only upper 4Cα. The axons of these cells preferentially target layer 3 interblobs. The other two cells have dendrites in lower 4Cα, extending into layer 4Cβ. They are therefore likely to receive P input, as well as input from M afferents that target lower 4Cα. Their axons arborize in both blobs and interblobs (Fig. 4*C*,*D*) but not 4B, similar to the axons of layer 4Cβ spiny stellates (Fig. 5, see below). They differ from layer 4Cβ cells, because many 4Cβ cells lack dendrites in layer 4Cα and therefore cannot sample from M afferents.

Quantitative analyses reveal the relationships between axonal projections and blobs for both types of lower 4Cα cells that have axons extending to layer 2/3. The two cells with stratified dendrites (Fig. 4*A*,*B*) contribute 2132 synaptic boutons to layer 2/3

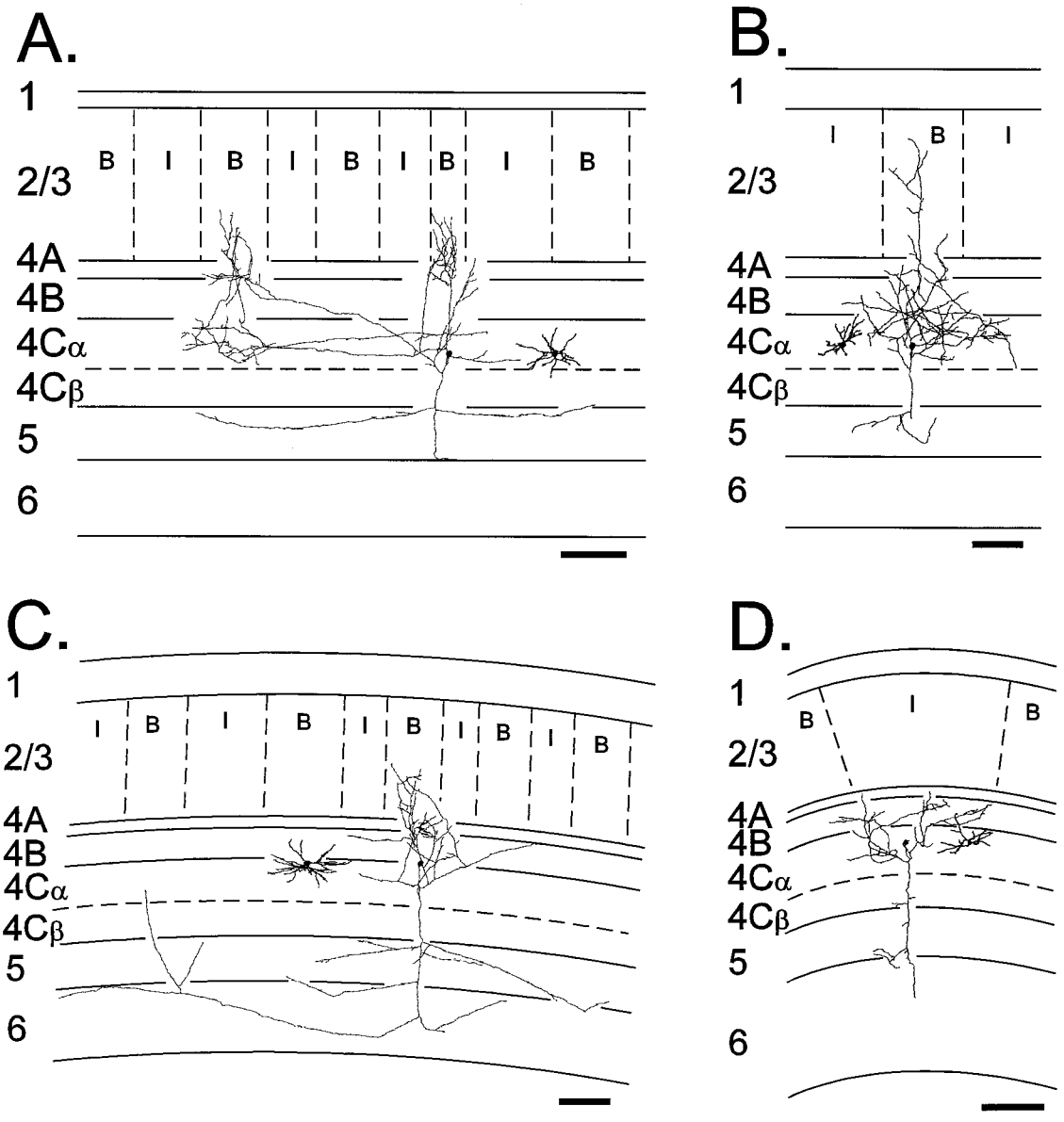

Figure 2. Reconstructions of the axonal and dendritic arbors of spiny stellate neurons, with somata in upper layer 4Cα and axonal arbors invading the superficial layers (layers 2–4B). All four cells (*A–D*) have substantial axonal arbors in layers 4B and 4Cα and weaker projections to deeper layers. The axonal arbors of cells *A–C* extend into layer 3, where they selectively target blobs. *Horizontal lines* indicate laminar boundaries, with the layers identified by the *numbers* and *letters* at the *left* of each *panel*. *Vertical dashed lines* indicate blob–interblob transitions, with blobs marked *B* and interblobs marked *I*. Axonal arbors are indicated by the *thinner*, *more extensive irregular lines* extending from the cell bodies, which are indicated by the *filled*, *approximately circular polygons*. The axonal arbors are shown in their actual positions relative to the laminar boundaries and CO blobs. So that axons and dendrites are not confused, dendritic arbors (*thicker lines* emanating from copies of the cell bodies) are shown shifted to one side from their actual positions. Cell bodies have been enlarged to make them more visible in the figures. Scale bars, 200 μm.

(1,066 boutons per cell). This is nearly fourfold more boutons per cell than upper 4Cα neurons contribute to layer 2/3. The distribution of boutons is clearly biased toward distances far from blob centers (Fig. 6*Biii*). More than half of the boutons are located >200 μm from a blob center, and more than 90% are >100 μm away. The two cells with dendrites extending into layer 4Cβ contribute 1574 synaptic boutons to layer 2/3 (787 per cell), and these are distributed uniformly across blobs and interblobs (Fig. 6*Biv*).

4Cβ neurons

All seven layer 4Cβ spiny stellate neurons in our sample have similar axonal and dendritic morphologies, regardless of the depth of the cell body within the layer or the distribution of dendrites relative to the 4Cα/4Cβ border. The dendrites of cells near the top of layer 4Cβ frequently cross into lower 4Cα (Fig. 5*A*), whereas cells deeper in 4Cβ restrict their dendrites to 4Cβ (Fig. 5*D*). No layer 4Cβ cells have dendrites extending into upper layer 4Cα. All seven cells have axons that extend through layer 4B and arborize in layers 3 and 4A, without any overall preference for blob versus interblob regions. Only two of the seven cells have axonal branches below layer 4C, and these are found in layer 6, not in layer 5. It is noteworthy that compared with layer 4Cα cells, the 4Cβ cells contribute similar numbers of boutons per cell within layer 4C, but these boutons are more evenly distributed

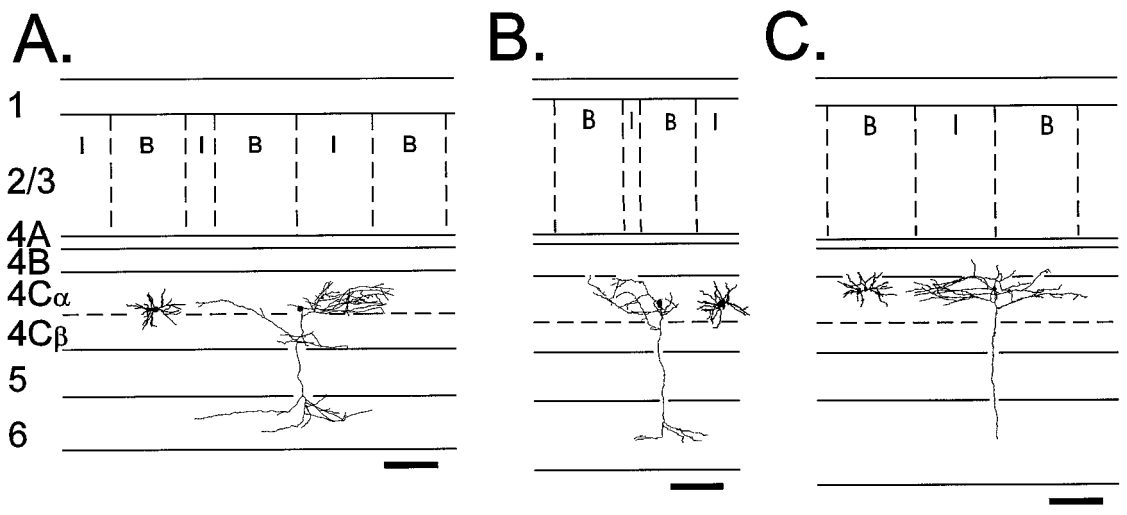

Figure 3. Reconstructions of the axonal and dendritic arbors of spiny stellate neurons, with somata in lower layer 4Cα (*A*) or upper layer 4Cα (*B*, *C*) and axonal arbors remaining primarily below layer 4B. The axonal arbors of these cells are primarily confined to layers 4C and 6. Cells with dendrites extending into layer 4Cβ have axonal arbors at the bottom of layer 4Cβ, as well as in layer 4Cα (*A*). Cells with dendrites only in layer 4Cα confine their layer 4C axonal arbors to 4Cα (*B*, *C*). Conventions are the same as in Figure 2. Scale bars, 200 μm.

between 4Cα and 4Cβ rather than focused on 4Cα (Fig. 6, compare *Aii* and *Av*).

Quantitative analyses of the synaptic boutons within layer 2/3 reveal their relatively high density and even distribution with respect to blobs. The layer 4Cβ spiny stellates contribute an average of 1378 layer 2/3 boutons per cell. This is close to five times the average number of boutons contributed to layer 2/3 by each upper 4Cα cell. About half of the layer 2/3 boutons from layer 4Cβ cells are located within 100 μm of a blob center, and the other half are more distant (Fig. 6*Bv*).

Despite the dispersion of the boutons of 4Cβ cells relative to blobs, their high density leads to a large contribution to both blob and interblob regions. For example, although upper 4Cα cells specifically target blobs in layer 2/3, they contribute a per cell average of only 230 boutons within 100 μm of blob centers, whereas 4Cβ cells each contribute 700 boutons per cell in the same region. Furthermore, there are more layer 4Cβ cells than 4Cα cells projecting axons to layer 2/3 for each square millimeter of cortical area (see below) (Beaulieu et al., 1992).

Relative contributions of M- and P-recipient neurons

We have estimated the relative synaptic contributions of each layer 4C cell type to layers 2/3 and 4B and the distributions of the layer 2/3 synapses relative to blobs. From these estimates, it is possible to quantitatively evaluate the contributions of M- versus P-recipient neurons. It is crucial to be aware that these estimates should not be considered to be indicative of the relative influences of the M and P pathways on each of the recipient zones. We are describing synaptic boutons from layer 4C spiny stellates only; synapses originating from other cell types, such as layer 4B neurons, also make substantial contributions with their own specific laminar and columnar distributions. It should also be kept in mind that not all synapses are likely to be functionally equivalent; synapses arising from one cell type might be stronger or weaker than those coming from another cell type (Stratford et al., 1996).

First, we must estimate the relative proportions of each of the cell types we have identified, assuming that inherent sampling biases and small sample sizes have not grossly skewed the sample. We estimate that approximately half of all layer 4C spiny stellate neurons are located in layer 4Cβ. This estimate is derived from the observation of Beaulieu et al. (1992) that there is a 1.4 times higher density of neurons in the lower versus upper half of layer 4C, combined with the observation that in our material the cell-dense zone corresponding to layer 4Cβ is only ~40% of the depth of layer 4C. We next assume that our small sample of neurons in lower 4Cα is representative of one-fifth of all 4Cα spiny stellate neurons (the region corresponds to 20% of the thickness of 4Cα; see above), or 10% of all layer 4C neurons. The remaining 40% of layer 4C neurons are represented by our sample of upper 4Cα neurons.

For each type of layer 4C spiny stellate, what percentage of all layer 4C spiny stellate cells do they constitute? For upper 4Cα cells, layer 2/3 boutons are contributed by 70% (7 of 10) of the cells. Seventy percent times 40% gives 28 as the percentage of all layer 4C cells represented by this population. Eighty percent of the upper 4Cα cells (32% of all layer 4C cells) project to layer 4B. Lower 4Cα contains three cell types, which together constitute 10% of layer 4C cells, or 3.3% for each cell type. The 4Cβ cells all have synaptic boutons in layers 2/3 and 4B, and these cells are half of all layer 4C spiny stellates.

We then estimate, for each cell type, the numbers of layer 2/3 and layer 4B boutons and the distributions of layer 2/3 boutons relative to blobs, contributed by a "typical" population of 100 layer 4C cells. For example, to determine the numbers of boutons in layer 4B or layer 2/3 from each cell type, the numbers of boutons per cell in the layer of interest (Fig. 6*A*) are multiplied by the weighting for the cell type (as calculated above). To determine the distributions of the layer 2/3 synapses from each cell type relative to blobs, the values are the average numbers of boutons per cell at each distance from blob centers (Fig. 6*B*) times the weighting for each cell type.

Layer 4B input

The overwhelming majority of synapses originating from layer 4C spiny stellates and terminating in layer 4B come from neurons in upper layer 4Cα. We estimate that a population of 100 layer 4C neurons provides 21,053 synaptic boutons to layer 4B. More than 80% of these (16,928 boutons, 80.4%) come from neurons in

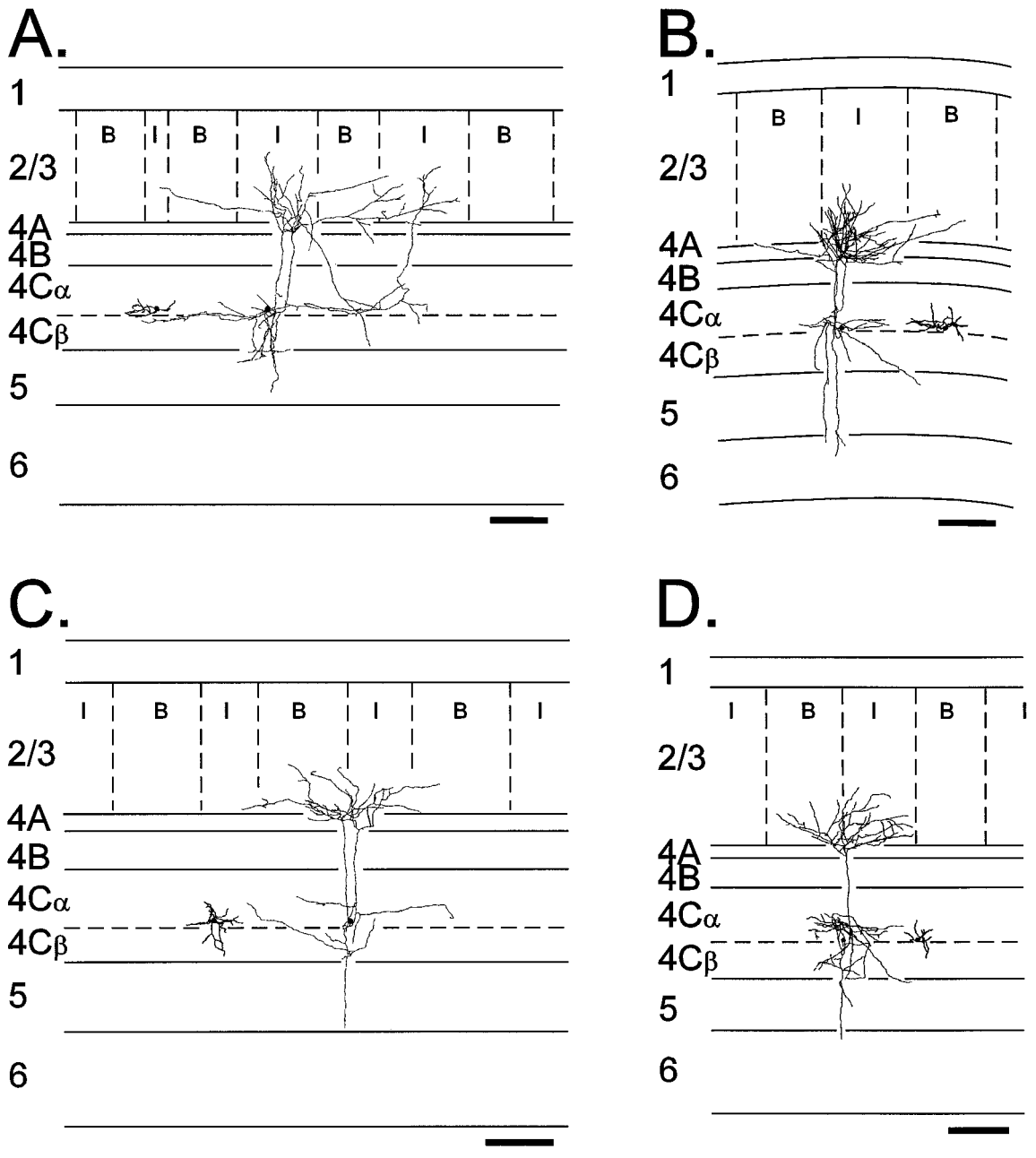

Figure 4. Reconstructions of the axonal and dendritic arbors of spiny stellate neurons, with somata in lower layer 4Cα and axons extending into layer 3. The cells in *A* and *B* have narrowly stratified dendritic arbors that are confined to lower 4Cα and do not extend into upper 4Cα or 4Cβ. The axonal arbors of these cells selectively target layer 3 interblobs. *C* and *D* illustrate cells with dendrites extending into layer 4Cβ. The axonal arbors of these cells target both blob and interblob regions of layer 3. Conventions are the same as in Figure 2. Scale bars, 200 μm.

upper layer 4Cα (529 boutons per cell × 32 cells). Only 3.2% of the synapses come from lower layer 4Cα neurons. The remaining 16.4% of the synapses come from the unbranched axons of layer 4Cβ spiny stellates as they pass through layer 4B (68.9 boutons per cell × 50 cells = 3445 boutons).

Layer 2/3 input

We estimate that 100 layer 4C spiny stellate neurons contribute 82,914 synapses to layer 2/3. Thus, the population of layer 4C neurons contributes approximately fourfold more synapses to layer 2/3 than to layer 4B (82,914 vs 21,053 boutons per 100 layer 4C spiny stellates). The majority of layer 2/3 synapses that come from layer 4C spiny stellates are from layer 4Cβ neurons. Layer 4Cβ cells contribute 68,883 (83.1%) of these synapses, which is nearly five times the remaining number (14,031) contributed by all the layer 4Cα cell types combined. Of the synapses contributed to layer 2/3 by layer 4Cα cells, (1) upper layer 4Cα cells contribute 7916 synapses (9.5% of the layer 2/3 boutons), (2) lower 4Cα cells with stratified dendrites contribute 3518 synapses (4.2%), and (3) lower 4Cα cells with dendrites in 4Cβ contribute 2597 synapses (3.1%).

The spatial distributions of the layer 2/3 synapses relative to blobs are illustrated in Figure 7. Figure 7*A* shows estimated numbers of synaptic boutons contributed by each cell type from a population of 100 layer 4C spiny stellate neurons. Figure 7*B*

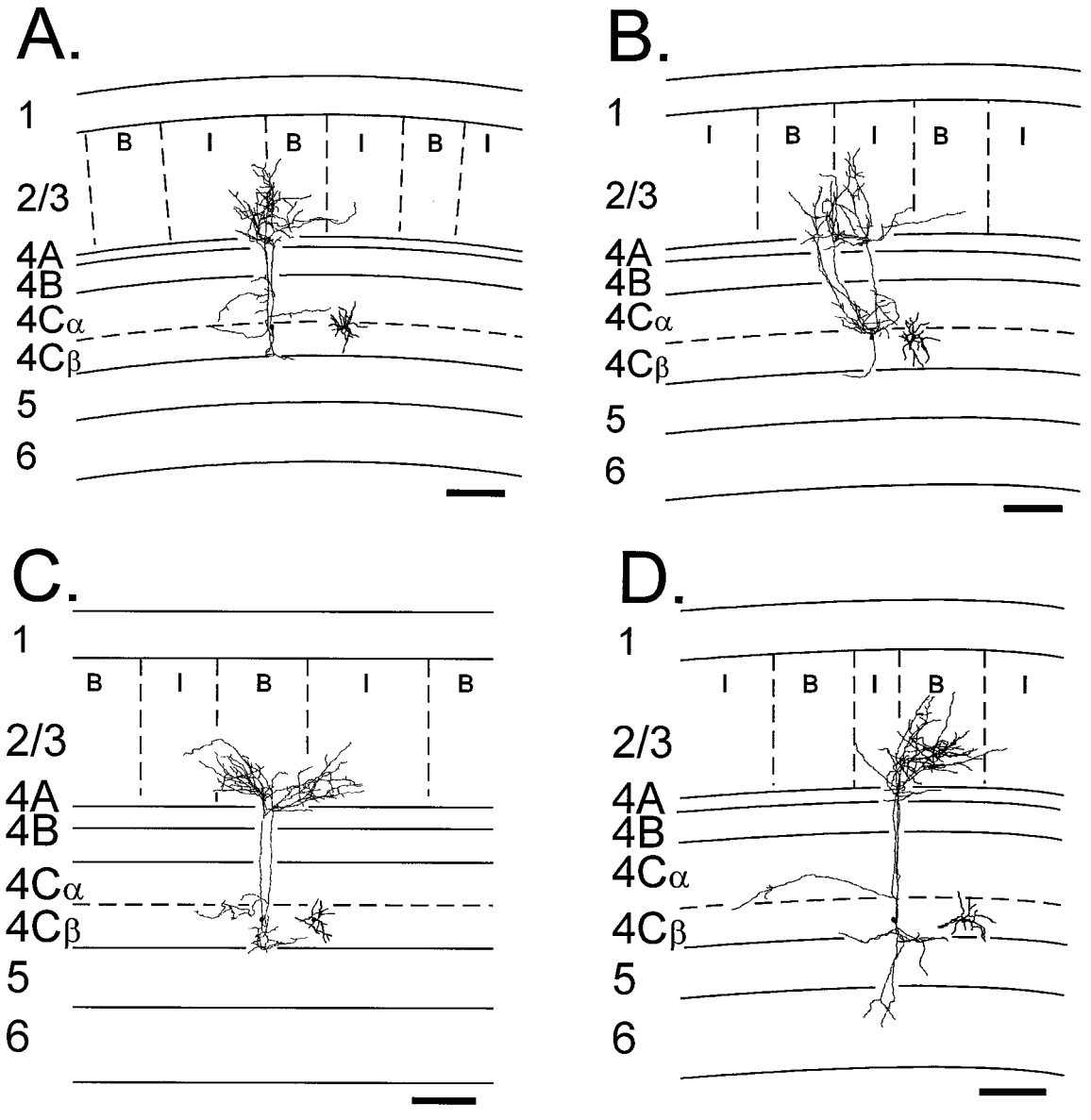

Figure 5. Reconstructions of the axonal and dendritic arbors of spiny stellate neurons, with somata in layer 4Cβ. The axonal arbors of these cells target both blobs and interblobs in layer 3, regardless of whether their dendrites extend into layer 4Cα (*A*, *B*) or remain confined to 4Cβ (*C*, *D*). Sparser axonal arbors are present in layer 4C and occasionally in deeper layers. Conventions are the same as in Figure 2. Scale bars, 200 μm.

illustrates the same data, except that the data in each bin of the histogram are expressed as a percentage of boutons from that bin only.

At all distances from blob centers, layer 4Cβ neurons contribute the great majority of synapses originating from layer 4C spiny stellate neurons. The percentage of synapses contributed by the 4Cβ cells is smallest at the extreme distances, very near to and very far from blob centers. At >200 μm from blob centers, 4Cβ cells contribute 67% of the synapses, and at <50 μm, they contribute 75%. These percentages increase at intermediate distances, peaking at 93% at 100–150 μm from blob centers.

The distribution of synapses contributed by layer 4Cα cells complements the 4Cβ cell distribution, peaking very far from blob centers (33% at >200 μm away) and also near to blob centers (25% at <50 μm). Within the population of 4Cα cells, upper 4Cα cells contribute most of the synapses near blob centers, whereas lower 4Cα cells contribute most of those far from blob centers.

DISCUSSION

The primate visual system is characterized by parallel pathways. In the retino–geniculo–cortical pathway, the M and P streams are distinct and well segregated. Extrastriate cortical areas (beyond V1) can be separated into a dorsal stream, specialized for analysis of spatial relationships and object motion, and a ventral stream, specialized for object identification (Desimone and Ungerlieder, 1989). The transient responses of M cells seem to be well suited for the production of motion-sensitive neurons, as found in the dorsal stream, whereas the small, color-opponent receptive fields of P neurons seem to be well suited to the later analysis of color and shape required for object identification in the ventral stream (Livingstone and Hubel, 1988). [A third system, the K stream,

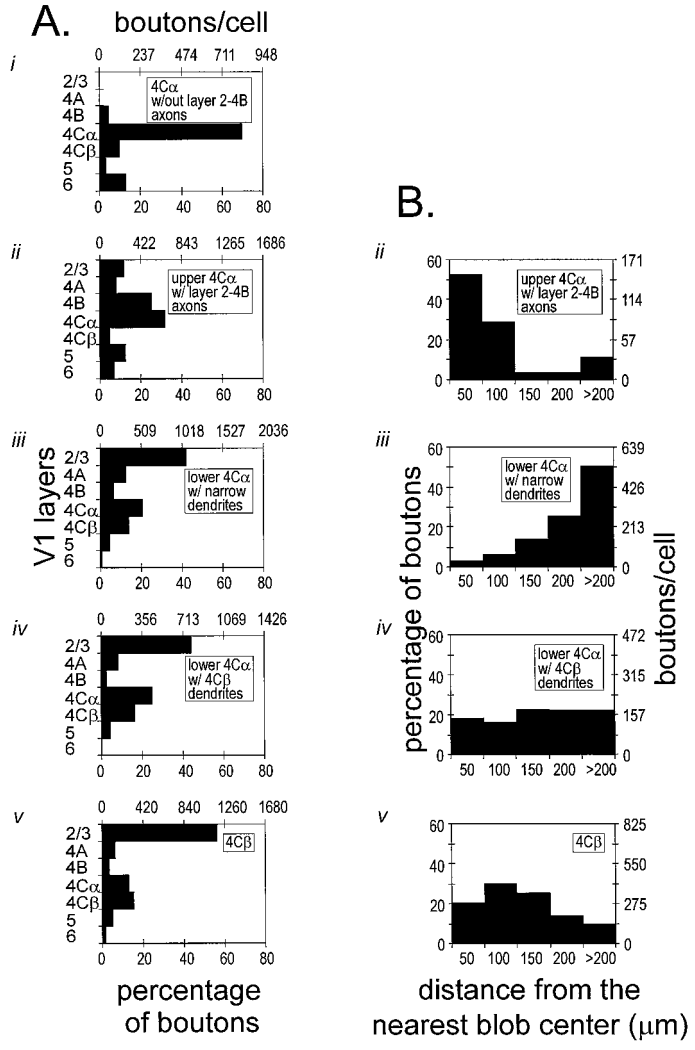

Figure 6. Histograms illustrating the laminar distributions (*A*) and columnar distributions relative to blobs (*B*) of synaptic boutons grouped according to five cell types (*i–v*): *i*, upper and lower layer 4Cα neurons without axons extending above layer 4C; *ii*, upper layer 4Cα neurons with axons extending above layer 4C; *iii*, lower 4Cα neurons with narrowly stratified dendrites and layer 3 axons; *iv*, lower 4Cα neurons with dendrites extending into layer 4Cβ and layer 3 axons; and *v*, layer 4Cβ neurons. In *A*, the synaptic boutons from all cells of a given type were pooled together and binned according to cortical layers, as indicated to the *left* of the histograms. The *axes* at the *bottom* of the histograms indicate the percentages of boutons from each cell type located within each layer. The *axes* at the *top* of the histograms indicate the numbers of boutons per cell located within each layer. The histograms in *B* illustrate the distributions relative to blob centers for synapses located within layer 2/3. The *numbers* at the *bottom* of each histogram indicate the upper limit of distances from blob centers for synapses counted in that bin. The *axes* at the *left* of the histograms indicate the percentages of boutons from each cell type located within each range of distances from their nearest blob center. The *axes* to the *right* indicate the numbers of boutons per cell located in each range of distances from blob centers.

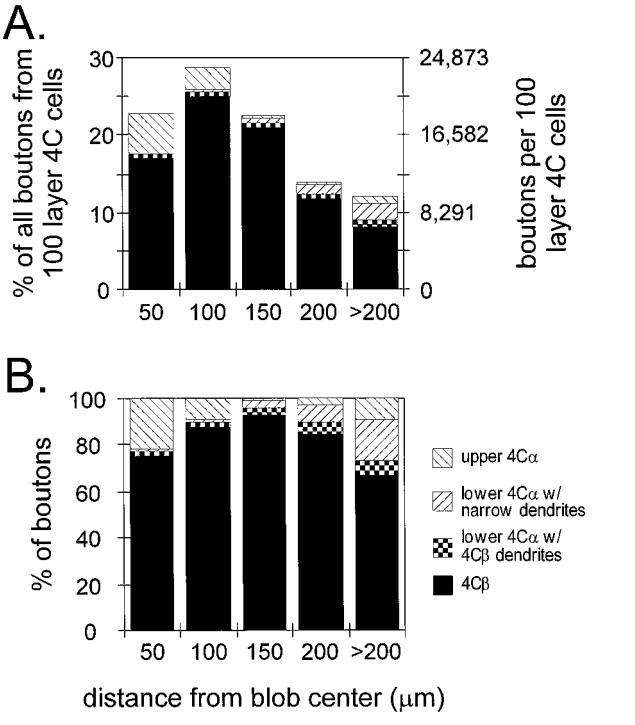

Figure 7. Histograms illustrating the relative synaptic contributions of each of four cell types (see legend at *right* of *B*) at various ranges of distances from blob centers in layer 2/3. In *A*, the *axis* to the *right* of the histogram corresponds to the estimated number of synaptic boutons contributed by a representative population of 100 layer 4C spiny stellate neurons (see Results). The *axis* to the *left* corresponds to the percentage of all boutons from all 100 cells. In *B*, the same bouton distributions are expressed as the percentage of boutons within each bin (range of distances from blob centers) of the histogram.

may also contribute importantly to color processing via its input directly to blobs (cf. Livingstone and Hubel, 1882, 1984; Casagrande, 1994; Hendry and Yoshioka, 1994; Martin et al., 1997).]

At a first approximation, our quantitative data support this notion. Layer 4B cells project to dorsal visual areas (for review, see Felleman and Van Essen, 1991), and the great majority of the input from layer 4C to layer 4B comes from M-recipient layer 4Cα neurons. Conversely, layer 3 cells project to ventral visual areas, and the overwhelming majority of their layer 4C input comes from P-recipient layer 4Cβ neurons.

M and P contributions to layer 3 neurons

Taken at face value, these observations might suggest that the M pathway has only a minor influence on layer 3, regardless of the location relative to blobs, but it is important to consider additional input from sources outside of layer 4C and possible differences in the functional influence of synapses from different cell types. Layer 4B neurons receive strong input from the M pathway and have dense axonal arbors, specifically in layer 2/3 blobs (Callaway and Wiser, 1996). Although the numbers of synapses from layer 4B cells have not been quantitatively analyzed, their blob-specific arbors appear similar in density and blob-specificity to upper 4Cα neurons. Blob-specific input to layer 3 also comes from K-type LGN afferents (Casagrande, 1994; Hendry and Yoshioka, 1994). Additional projections to layer 3 arise from neurons in layers 4A, 5, and 6 (Callaway and Wiser, 1996; Wiser and Callaway, 1996). The contribution from layer 5 is particularly dense, and we report here that this layer receives input from the M-recipient layer 4Cα but not from 4Cβ. Likely, functional differences in the input from these disparate sources make it still more difficult to estimate the relative contributions of the M and P (and K) pathways to layer 3. However, it appears likely that the influence of the M pathway is greater than suggested by simply counting synapses. For example, inactivation of M layers of the LGN can profoundly reduce visual activation of layer 2/3 neu-

rons, irrespective of their position relative to blobs (Nealey and Maunsell, 1994). The spatial frequency and contrast sensitivities of neurons in layer 3 blobs are also suggestive of a strong M contribution (Edwards et al., 1995).

M and P contributions to layer 4B neurons

Just as the relatively strong input from layer 4Cβ to layer 3 should not be taken as an indication that layer 3 lacks M input, one should not assume that a lack of projections from 4Cβ cells to layer 4B implies that layer 4B cells are not influenced by the P stream. Photostimulation studies have revealed substantial excitatory synaptic input from layer 4Cβ neurons onto layer 4B pyramidal cells (Sawatari and Callaway, 1996). For some cells, there appeared to be as much input from 4Cβ as from 4Cα, but in the present study, we find that upper 4Cα cells provide five times more synapses to layer 4B than 4Cβ cells. Thus, much of the input from 4Cβ cells onto layer 4B neurons is likely to be located on apical dendrites of pyramidal neurons. The surprisingly high density of layer 2/3 synapses that come from layer 4Cβ neurons argues that their synapses onto apical dendrites of layer 4B pyramidal neurons could be numerous. We estimate that 4Cβ cells contribute four times more synapses to layer 3 than 4Cα cells contribute to layer 4B. Synapses localized to apical dendrites might, however, have a less direct functional influence *in vivo*, which is not apparent from the measurement of synaptic responses *in vitro*.

M and P contributions to blobs and interblobs

Within layer 2/3, we have further characterized the relationships of M and P pathways to blob versus interblob regions. The laminar patterns of dendritic arbors of individual layer 4C spiny stellate neurons reveal the likely contributions of M and P afferents to their input. The patterns of axonal arborization relative to extrastriate projection neurons in the CO blobs and interblobs of layer 2/3 provide insight into the likely contributions of the same M- and P-recipient neurons to higher cortical areas.

We find that neurons with dendrites in the upper part of layer 4Cα have axonal arbors in layer 4B and the CO blobs of layer 2/3 but rarely in interblobs, but some neurons, with somata deeper in layer 4Cα, lack dendritic branches in upper 4Cα and provide dense input to CO interblob regions. The layer 4Cα spiny stellates providing this interblob input are of two types: (1) cells with narrowly stratified dendrites restricted to lower 4Cα and dense axonal arbors specific for interblobs; (2) cells with dendritic branches in lower 4Cα and 4Cβ, whose axons target both blobs and interblobs. Layer 4Cβ spiny stellates have extremely dense axonal arbors in both blobs and interblobs but not layer 4B. Some of these 4Cβ neurons have dendritic branches in lower 4Cα and can therefore sample M input, as well as P input.

These findings point out the importance of considering possible subdivisions of layer 4C beyond the traditional 4Cα–4Cβ distinction. Most notably, the middle of layer 4C (lower 4Cα) appears to play an unique role in visual information processing. This has been emphasized previously by the experimental findings and observations of Lund and colleagues (cf. Blasdel and Lund, 1983; Mates and Lund, 1983; Yoshioka et al., 1994). Our findings provide a clearer view of how the dendritic arbors of individual spiny stellate neurons in this region are related to their patterns of axonal arborization.

We find that neurons in the bottom of layer 4Cα make substantial axonal projections to interblobs. These cells presumably provide M input to interblobs. Outside of this zone, our reconstructions of neurons in upper layer 4Cα and in layer 4Cβ are primarily in keeping with expectations from the retrograde labeling studies of Lachica et al. (1992) (but see Yoshioka et al., 1994). Upper 4Cα neurons provide input to layer 4B and to layer 3 blobs but relatively little input to interblobs. Layer 4Cβ neurons provide strong input to blobs and interblobs but much less to layer 4B.

In considering the possibility of M input to interblobs, it is important to emphasize that layer 4C cells with axons projecting to interblobs only rarely have dendrites in upper layer 4Cα. This is a crucial point, because there appear to be two types of M afferents, one that targets only upper layer 4Cα and another that innervates the whole depth of layer 4Cα (Blasdel and Lund, 1983). The cells connecting to interblobs therefore cannot receive input from the subset of LGN M afferents whose axons only invade upper 4Cα (Blasdel and Lund, 1983). Instead, an M contribution to interblobs appears to arise from the M afferents that target both upper and lower 4Cα. The 4Cα cells specifically targeting blobs and layer 4B, on the other hand, do have substantial dendritic branches in upper 4Cα and are therefore likely to relay input from both types of M afferents. These observations suggest that both blobs and interblobs receive contributions from the M pathway, as implied previously by inactivation studies (Nealy and Maunsell, 1994). This arrangement also helps to explain why many neurons in interblobs, like blob cells, have relatively low optimal spatial frequencies, despite the general trend for higher frequencies farther from blobs (Edwards et al., 1995). Functional differences between blobs and interblobs appear to be attributable in part to functional differences between the type of M input to the two regions rather than a lack of M input to interblobs.

Functional implications

Consideration of the functional differences between the various types of geniculate afferents is therefore important for interpreting the functional implications of the present findings. The primate retina and LGN are characterized by many functionally and anatomically distinct types of neurons (for review, see Casagrande and Norton, 1991; Casagrande, 1994). Prominent among these are the M and P cells, which constitute the M and P retino–geniculo–cortical pathways. P cells in the retina and LGN are characterized by color-opponent receptive fields, sustained visual responses, tuning to high spatial frequencies, and poor luminance contrast sensitivity. M cells are characterized by a lack of wavelength selectivity, transient visual responses, tuning to low spatial frequencies, and high luminance contrast sensitivity. M cells can be further subdivided based on the linearity of spatial summation within their receptive fields. Linear M cells ($\sim$75% of all M cells in the LGN) have receptive fields that are remarkably similar to X cells in the cat and can therefore be referred to as M_X. Nonlinear M cells are like cat Y cells and can be referred to as M_Y (Kaplan and Shapley, 1982; Shapley and Perry, 1986). P cells are linear but otherwise bear relatively little functional similarity to either X or Y cells in cats.

Because the most striking difference among M cells is the M_X versus M_Y distinction, it is natural to guess that this difference correlates with the variation in laminar specificity of M afferents. We speculate that the M afferents projecting exclusively to upper layer 4Cα are of the M_Y variety, whereas those projecting throughout 4Cα are M_X. The basis for this speculation is the possible homology between M_X and M_Y cells and X and Y cells in the cat. The remarkable functional similarities between these cell types suggest that the M-recipient layer 4Cα in the primate

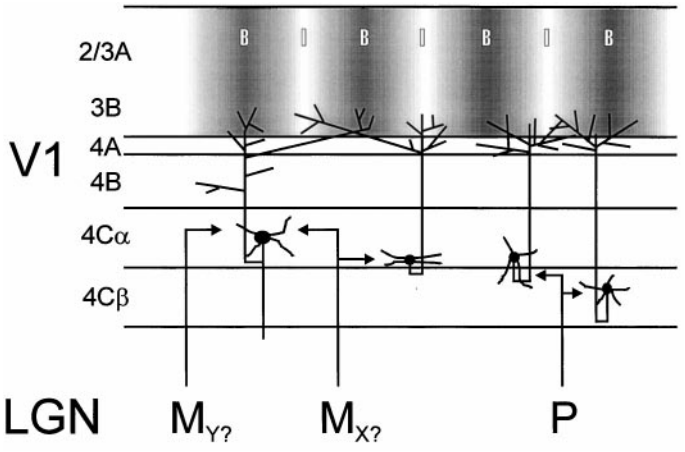

Figure 8. Schematic diagram illustrating four types of layer 4C spiny stellate neurons that project axons to layer 3, the relationships of their dendritic arbors to M and P afferents from the LGN, and the relationships of their axonal arbors to laminar boundaries and to CO blobs in layer 3. The *far left* of the four cell types has dendrites confined to layer 4Cα, where it presumably receives input from LGN M afferents but not P afferents. We speculate that such input comes both from M_Y afferents targeting only upper layer 4Cα and M_X afferents targeting upper and lower 4Cα. The axons of this cell type arborize in layers 4A and 4B and layer 3 blobs. The next cell type from the *left* (*middle left*) has narrowly stratified dendrites confined to lower layer 4Cα. We speculate that it receives input from M_X but not M_Y or P LGN afferents. The axons of this cell type arborize preferentially in layer 3 interblobs. The next cell type (*middle right*) is located in lower layer 4Cα and has dendrites in lower 4Cα and in 4Cβ. We suggest that these cells receive input from M_X and P afferents but not M_Y afferents. The axons of these cells arborize in layer 4A and layer 3 blobs and interblobs. The last cell type (*far right*) is found in layer 4Cβ. These cells either have dendrites confined to layer 4Cβ and receive just P input (as illustrated) or also have dendrites extending into lower 4Cα, where they might receive M_X input. The axons of these cells arborize in layer 4A and layer 3 blobs and interblobs. *Horizontal lines* indicate laminar boundaries, with layers identified to the *left*. *Darker shaded regions* in layer 2/3 indicate blobs (*B*), and *lighter regions* indicate interblobs (*I*).

might be organized like layer 4 of the cat. In cat area 17, geniculate Y cells usually innervate just upper layer 4, whereas X cells innervate its entire depth (Ferster and LeVay, 1978; Gilbert and Wiesel, 1979; Humphrey et al., 1985).

If our speculation is correct, what are the implications? Because we find that neurons with dendrites in lower 4Cα project to interblobs and those with dendrites in upper 4Cα project to blobs, we suggest that blobs are influenced by both the M_X and M_Y pathways, whereas interblobs are influenced by just the linear M_X pathway (Fig. 8). Because the only other input to interblobs would be from layer 4Cβ cells receiving linear P input, we suggest that interblobs receive only linear input. Furthermore, neurons receiving exclusively M_X input and no P input (those with narrowly stratified dendrites) provide output exclusively to interblobs. Thus, any properties unique to these cells would not be transmitted to blobs or layer 4B. Conversely, properties unique to upper layer 4Cα neurons receiving both M_X and M_Y input would be transmitted to layer 4B and to blobs but not to interblobs (Fig. 8).

These relationships suggest a further similarity between the cat and monkey systems. In area 17 of cats, blobs receive direct input from nonlinear Y cells (Shoham et al., 1997). Thus, the two species may have in common a linear interblob system interrupted by blobs that also receive nonlinear Y or M_Y input. Perhaps upper layer 4 in cats also projects specifically to blobs.

Further studies will be required to gain still greater understanding of the roles of each type of layer 4C spiny stellate neurons in visual information processing. *In vivo* studies correlating receptive field properties to the anatomical properties we have described here would be particularly useful. Similar studies relating the visual responses of LGN neurons to their laminar patterns of axonal termination in V1 (i.e., upper vs lower 4Cα) will also provide significant insight.

REFERENCES

Beaulieu C, Kisvardy Z, Somogyi P, Cynader M, Cowey A (1992) Quantitative distribution of GABA-immunopositive and -immunonegative neurons and synapses in the monkey striate cortex (Area 17). Cereb Cortex 2:295–309.

Blasdel GG, Fitzpatrick D (1984) Physiological organization of layer 4 in macaque striate cortex. J Neurosci 4:880–895.

Blasdel GG, Lund JS (1983) Termination of afferent axons in macaque striate cortex. J Neurosci 3:1389–1413.

Callaway EM (1998) Local circuits in primary visual cortex of the macaque monkey. Annu Rev Neurosci 21:47–74.

Callaway EM, Wiser AK (1996) Contributions of individual layer 2–5 spiny neurons to local circuits in macaque primary visual cortex. Vis Neurosci 13:907–922.

Casagrande VA (1994) A third parallel visual pathway to primate area V1. Trends Neurosci 17:305–310.

Casagrande VA, Norton TT (1991) Lateral geniculate nucleus: a review of its physiology and function. In: Vision and visual dysfunction: the neural basis of visual function, Vol 4 (AG Leventhal, ed), pp 41–84. New York: Macmillan.

Desimone R, Ungerleider L (1989) Neural mechanisms of visual processing in monkeys. In: Handbook of neuropsychology, Vol 2 (Boller F, Grafman J, eds), pp 267–299. Amsterdam: Elsevier.

Edwards DP, Purpura KP, Kaplan E (1995) Contrast sensitivity and spatial frequency response of primate cortical neurons in and around the cytochrome oxidase blobs. Vision Res 35:1501–1523.

Felleman DJ, Van Essen DC (1991) Distributed hierarchical processing in the primate cerebral cortex. Cereb Cortex 1:1–47.

Ferster D, LeVay S (1978) The axonal arborizations of lateral geniculate neurons in the striate cortex of the cat. J Comp Neurol 182:923–944.

Gilbert CD, Wiesel TN (1979) Morphology and intracortical projections of functionally characterized neurones in the cat visual cortex. Nature 280:120–125.

Hendrickson AE, Wilson JR, Ogren MP (1978) The neuroanatomical organization of pathways between the dorsal lateral geniculate nucleus and visual cortex in Old World and New World primates. J Comp Neurol 182:123–136.

Hendry SH, Yoshioka T (1994) A neurochemically distinct third channel in the macaque dorsal lateral geniculate nucleus. Science 264:575–577.

Hubel DH, Wiesel TN (1972) Laminar and columnar distribution of geniculo-cortical fibers in the macaque monkey. J Comp Neurol 146:421–450.

Humphrey AL, Sur M, Uhlrich DJ, Sherman SM (1985) Projection patterns of individual X- and Y-cell axons from the lateral geniculate nucleus to cortical area 17 in the cat. J Comp Neurol 233:159–189.

Kaplan E, Shapley RM (1982) X and Y cells in the lateral geniculate nucleus of macaque monkeys. J Physiol (Lond) 330:125–143.

Lachica EA, Beck PD, Casagrande VA (1992) Parallel pathways in macaque monkey striate cortex: anatomically defined columns in layer III. Proc Natl Acad Sci USA 89:3566–3570.

Livingstone M, Hubel D (1988) Segregation of form, color, movement, and depth: anatomy, physiology, and perception. Science 240:740–749.

Livingstone MS, Hubel DH (1982) Thalamic inputs to cytochrome oxidase-rich regions in monkey visual cortex. Proc Natl Acad Sci USA 79:6098–6101.

Livingstone MS, Hubel DH (1984) Anatomy and physiology of a color system in the primate visual cortex. J Neurosci 4:309–356.

Martin PR, White AJ, Goodchild AK, Wilder HD, Sefton AE (1997) Evidence that blue-on cells are part of the third geniculocortical pathway in primates. Eur J Neurosci 9:1536–1541.

Mates SL, Lund JS (1983) Neuronal composition and development in lamina 4C of monkey striate cortex. J Comp Neurol 221:60–90.

Merigan WH, Maunsell JHR (1993) How parallel are the visual pathways? Annu Rev Neurosci 16:369–402.

Nealey TA, Maunsell JHR (1994) Magnocellular and parvocellular contributions to the responses of neurons in macaque striate cortex. J Neurosci 14:2069–2079.

Sawatari A, Callaway EM (1996) Convergence of magno- and parvocellular pathways in layer 4B of macaque primary visual cortex. Nature 380:442–446.

Shapley R, Perry VH (1986) Cat and monkey retinal ganglion cells and their visual functional roles. Trends Neurosci 9:229–235.

Shoham D, Hubener M, Schulze S, Grinvald A, Bonhoeffer T (1997) Spatio-temporal frequency domains and their relation to cytochrome oxidase staining in cat visual cortex. Nature 385:529–533.

Stratford KJ, Tarczy-Hornoch K, Martin KAC, Bannister NJ, Jack JJ (1996) Excitatory synaptic inputs to spiny stellate cells in cat visual cortex. Nature 382:258–261.

Tootell RB, Hamilton S, Silverman MS, Switkes E (1988a) Functional anatomy of macaque striate cortex. I. Ocular dominance, binocular interactions, and baseline conditions. J Neurosci 8:1500–1530.

Tootell RB, Hamilton S, Switkes E (1988b) Functional anatomy of macaque striate cortex. IV. Contrast and magno-parvo streams. J Neurosci 8:1594–1609.

Tootell RB, Silverman MS, Hamilton S, Switkes E, De Valois RL (1988c) Functional anatomy of macaque striate cortex. V. Spatial frequency. J Neurosci 8:1610–1624.

Wiser AK, Callaway EM (1996) Contributions of individual layer 6 pyramidal neurons to local circuitry in macaque primary visual cortex. J Neurosci 16:2724–2739.

Yabuta NH, Callaway EM (1998) Cytochrome oxidase blobs and intrinsic horizontal connections of layer 2/3 pyramidal neurons in primate V1. Vis Neurosci, in press.

Yoshioka T, Levitt JB, Lund JS (1994) Independence and merger of thalamocortical channels within macaque monkey primary visual cortex: anatomy of interlaminar projections. Vis Neurosci 11:467–489.